IEEE Photonics Journal
An IEEE Photonics Society Publication

Open Access

Adaptive Optimization of Quantized Perturbation Coefficients for Fiber Nonlinearity Compensation

Volume 8, Number 3, June 2016

M. Malekiha
D. V. Plant, Fellow, IEEE

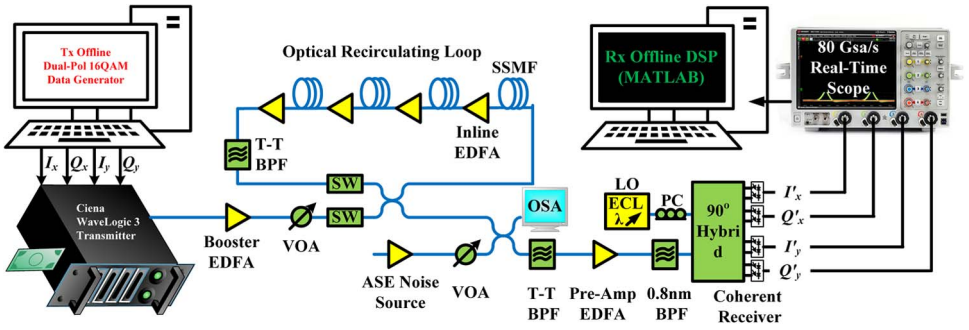

DOI: 10.1109/JPHOT.2016.2566341
1943-0655 © 2016 IEEE

IEEE photonics SOCIETY

IEEE

Adaptive Optimization of Quantized Perturbation Coefficients for Fiber Nonlinearity Compensation

M. Malekiha and D. V. Plant, *Fellow, IEEE*

Department of Electrical and Computer Engineering, McGill University, Montreal, QC H3A 0E9, Canada

DOI: 10.1109/JPHOT.2016.2566341

Manuscript received March 29, 2016; revised May 3, 2016; accepted May 6, 2016. Date of publication May 10, 2016; date of current version May 26, 2016. Corresponding author: M. Malekiha (e-mail: mahdi.malekiha@gmail.com).

Abstract: In the perturbation-based nonlinearity compensation (PB-NLC) technique, quantization of perturbation coefficients is employed for reduction of computational and implementation complexity. In this paper, we propose and experimentally verify the adoption of a decision-directed least mean square algorithm for optimization and complexity reduction of PB-NLC equalizer. We show that for 32-GBaud dual polarization 16-QAM after 2560 km of single-mode fiber, the proposed scheme further reduces the computational term by 46%, compared with that of conventional PB-NLC with uniform quantization of perturbation coefficients for the same Q-factor improvement.

Index Terms: Fiber optics communications, coherent communications, fiber nonlinearity, perturbation theory.

1. Introduction

Mitigating the effects of fiber nonlinearities is one of the key requirements for achieving higher channel capacities in coherent optical transmission systems. These nonlinearities limit achievable transmission distances, and therefore, nonlinearity compensation becomes crucial for 400 G/1 T transmission systems [1]. Digital back propagation (DBP) has been proposed for intra-channel nonlinearity compensation [2]. DBP normally requires multiple computation steps per fiber span and at least two samples per symbol for optimum nonlinearity compensation all of which can lead to high computational complexity in long haul dispersion-unmanaged fiber optic systems [3]. Alternatively, recently proposed PB-NLC techniques may compensate accumulated nonlinear effects with only one computation step and these techniques can be implemented with one sample per symbol [4]. However, practical implementation of this technique is limited due to the excessively large number of perturbation terms. This is especially true in dispersion-unmanaged links where numerous perturbation terms have to be considered due to the long dispersion induced delay spread of the pulses. While quantization of the perturbation reduces the computational complexity, fewer quantization levels leads to reduced performance. Recently, MMSE-based quantization schemes demonstrated the possibility of using only three distinct levels for perturbation coefficients. However, these levels are determined offline using an exhaustive search approach [5]. These days, with fast network expansion and adaptation of the dynamic optical networking, there is a possibility for numerous alternate paths for the propagating signal, where

each path may bear a different set of perturbation coefficients. Thus, identification of the correct set of perturbation coefficients becomes a very difficult task in meshed optical networks.

Low complexity adaptive nonlinear equalization algorithms are highly desirable for next generation agile and flexible rate fiber optic communication systems. To achieve this, we recently proposed a novel adaptive nonlinear equalizer [6]. In this paper, based on our previous work, we improve the performance of the quantized PB-NLC technique and reduce its computational complexity. To achieve this, we start with the regular calculations of the perturbation terms, employing low accuracy and large step size. After linear quantization of the perturbation coefficients, values in the middle of each interval are then used as starting points for the DD-LMS algorithm which is required in order to optimize and minimize the quantization error. Using this approach, with only five quantized terms, we show Q-factor improvement of 1.8 dB for 2560 km of SMF transmission, in comparison to the linear compensation only.

2. Principle of Perturbation Based Nonlinearity Compensation

The evolution of optical field envelope in a fiber optic link is described by the nonlinear Schrodinger equation [7]

$$\frac{\partial}{\partial z}u(t,z)+j\frac{\beta_2(z)}{2}\frac{\partial^2}{\partial t^2}u(t,z)=j\gamma(z)|u(t,z)|^2u(t,z) \tag{1}$$

where $u(t,z)$ is the optical field, $\beta_2(z)$ is the group velocity dispersion, and $\gamma(z)$ is the nonlinear coefficient. The nonlinear term in (1) can be treated as a small perturbation by denoting $u(t,z)=u_0(t,z)+j\Delta u(t,z)$, where $u_0(t,z)$ is the solution of linear propagation and $\Delta u(t,z)$ is the perturbation due to the nonlinear effects. Under the first-order approximation, the intra-channel four wave mixing (IFWM) induced nonlinear distortion on the transmitted symbol can be expressed as [8]

$$\Delta A_{0,x}=P^{\frac{3}{2}}\sum_{\forall m\neq 0,n\neq 0}C_{m,n}\left(A_{n,x}A^*_{m+n,x}A_{m,x}+A_{n,y}A^*_{m+n,y}A_{m,x}\right) \tag{2}$$

$$\Delta A_{0,y}=P^{\frac{3}{2}}\sum_{\forall m\neq 0,n\neq 0}C_{m,n}\left(A_{n,y}A^*_{m+n,y}A_{m,y}+A_{n,x}A^*_{m+n,x}A_{m,y}\right). \tag{3}$$

Here, x and y subscripts denote the two polarizations, P is the optical signal power, $C_{m,n}$ is the perturbation coefficient with m and n denoting the symbol index relative to the current symbol. $A_{k,x/y}$ is the transmitted symbol. Equations (2) and (3) imply that the nonlinear field is a linear combination of transmitted symbol triplets, weighted by $C_{m,n}$ coefficients. For Gaussian pulses and a lossless medium, analytical expressions expressed in terms of the exponential integral function exist for the nonlinear perturbation coefficients. For other pulse shapes, they can be numerically evaluated as follows [9]:

$$C_{m,n}=ik\int_o^L dz\gamma(z)f(z)\times\int dt g^{(0)*}(z,t)g^{(0)}(z,t-mT)g^{(0)}(z,t-nT)g^{(0)*}(z,t-(n+m)T). \tag{4}$$

Here, $\gamma(z)$ denotes the fiber nonlinear coefficient, k is the scaling factor $f(z)$ which describes the power distribution profile along the link, T stands for the symbol period, $g^{(0)}(0,t)$ is the pulse shape with zero accumulated dispersion $(z=0)$, and $g^{(0)}(z,t)$ is the dispersed pulse shape corresponding to a fiber length z which is calculated according to

$$g^{(0)}(z,t)=ifft\left\{fft\left[g^{(0)}(0,t)\right]\times\exp\left[-i\beta_2(2\pi f)^2z/2\right]\right\}. \tag{5}$$

$(i)fft[\cdot]$ denotes the (inverse) Fourier transform, f is frequency, and β_2 is the first-order group velocity dispersion [9].

In order to reduce the complexity of (2) and (3) quantization of perturbation coefficients (i.e., combining multiple terms with similar perturbation coefficients to reduce the number of complex multiplications) has been proposed [6]. In this case, (2) and (3) can be simplified as

$$\Delta A_{0,x} = P^{\frac{3}{2}} \sum_{k=1}^{N_k} C_k \sum_{\forall m,n \in C_k} \left(A_{n,x} A^*_{m+n,x} A_{m,x} + A_{n,y} A^*_{m+n,y} A_{m,x} \right) \tag{6}$$

$$\Delta A_{0,y} = P^{\frac{3}{2}} \sum_{k=1}^{N_k} C_k \sum_{\forall m,n \in C_k} \left(A_{n,y} A^*_{m+n,y} A_{m,y} + A_{n,x} A^*_{m+n,x} A_{m,y} \right) \tag{7}$$

where N_k is number of quantization levels, and the region representative C_k was obtained using the following formula:

$$m, n \in C_k \quad \text{if} \quad C_{k,\text{lower}} \leq C_{m,n} \leq C_{k,\text{upper}}$$
$$C_k = \frac{C_{k,\text{upper}} + C_{k,\text{lower}}}{2}. \tag{8}$$

Unfortunately, conventional uniform quantization does not provide optimum performance and therefore optimized quantization levels and quantized values have to be determined [5]. The exhaustive search method with the minimum mean square error (MMSE) as the criteria has been proposed for off-line calculation of optimum quantized perturbation coefficients and the corresponding quantization levels [5]. However, this approach has a limited practical use when it comes to reconfigurable mesh optical networks.

3. Optimization of Quantized Perturbation Coefficients

In this work, we further investigate the quantization of perturbation coefficients and propose a novel nonlinearity compensator/equalizer based on adaptive quantization of perturbation coefficients instead of using the average value for each quantization region as per (8). For this purpose, we use the DD-LMS algorithm to refine these values, which improves the performance. Rephrasing (6) and (7), equalized symbols can be express as

$$A_x^{\text{out}} = A_x + C_1 \Gamma_{x,1} + C_2 \Gamma_{x,2} + \cdots \tag{9}$$

$$A_y^{\text{out}} = A_y + C_1 \Gamma_{y,1} + C_2 \Gamma_{y,2} + \cdots \tag{10}$$

where we define

$$\Gamma_{x,k} = \sum_{m,n \in C_k} \left(A_{n,x} A^*_{m+n,x} A_{m,x} + A_{n,y} A^*_{m+n,y} A_{m,x} \right) \tag{11}$$

$$\Gamma_{y,k} = \sum_{m,n \in C_k} \left(A_{n,y} A^*_{m+n,y} A_{m,y} + A_{n,x} A^*_{m+n,x} A_{m,y} \right). \tag{12}$$

Each C_k is continuously updated based on the stochastic gradient algorithm, using the following set of equations:

$$C_{k,x}(p+1) = C_k(p) + \mu \varepsilon_{k,x}(p) \Gamma^*_{x,k}(k) \tag{13}$$

$$C_{k,y}(p+1) = C_k(p) + \mu \varepsilon_{k,y}(p) \Gamma^*_{y,k}(k). \tag{14}$$

Here, μ is the algorithm step size, p denotes the update step index, and $\varepsilon_{k,x/y}$ is the error at pth step, which is given by

$$\varepsilon_{\substack{x \\ y}}(p) = A^{\text{out}}_{\substack{x \\ y}}(p) - \text{decision}\left\{ A^{\text{out}}_{\substack{x \\ y}}(p) \right\}. \tag{15}$$

We point out in the absence of noise based on (2) and (3), and we have

$$C_{k,x} = C_{k,y}. \tag{16}$$

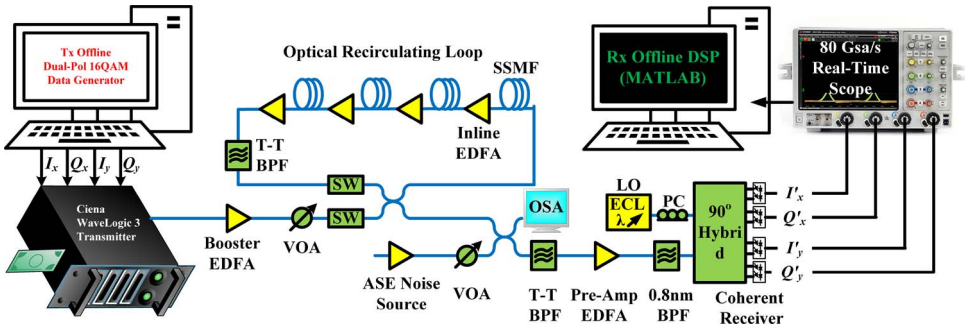

Fig. 1. Experimental setup. EDFA: Erbium-doped fiber amplifiers; BPF: Band-pass filter; T-T BPF: Tunable bandwidth and tunable center frequency band-pass filter; LO: Local oscillator; PC: Polarization controller; SW: Switch.

Therefore, (13) and (14) can be averaged over two polarizations for better estimation and higher noise rejection. Alternatively, for a more efficient implementation, the adaptation process can be divided between two polarizations where half of the coefficients are updated using the X-polarization, and the remaining coefficients are calculated using the Y-polarization.

4. Experimental Setup

Fig. 1 shows the schematic diagram of the experimental setup. On the transmitter side offline DSP, four 2-tuple independent pseudo-random bit sequences are mapped to 16-QAM symbols, followed by pulse shaping at two samples per symbol for each polarization. A Ciena WaveLogic 3 (WL3) line card was employed, which contains four 39.5 GSa/s 6 bit digital-to-analog converters (DACs), a tunable frequency laser source, and a dual-polarization (DP) IQ-modulator. The transmitter laser was operating at 1554.94 nm. The transmitter analog frequency response is compensated using the on-board built-in DSP of the WL3. The output optical signal is then boosted to 23 dBm using an erbium-doped fiber amplifier (EDFA), and subsequently attenuated using a conventional variable optical attenuator (VOA) in order to get a desired optical launch power. The optical signal is then launched into a recirculating loop. This loop consists of four spans of 80 km of single mode fiber (SMF-28e+LL) and four inline EDFAs. Each inline EDFA has a noise figure of 5.5 dB. A tunable bandwidth and tunable center wavelength band-pass filter (T-T BPF) is inserted after the fourth span in order to reject out-of-band amplified spontaneous emission (ASE) noise accumulated during transmission. The gain of the last EDFA is adjusted (increased by 10 dB compared to the other EDFAs) in order to compensate for losses occurring inside the recirculating loop, including switches, couplers and the band-pass filter.

At the receiver side, the gain of the pre-amplifier EDFA was adjusted to ensure that the signal power reaching the coherent receiver was held constant at 5 dBm. Finally, a 0.8 nm BPF was used to filter out the out-of-band amplified spontaneous emission noise generated by the pre-amplifier. At the polarization-diversity 90° optical hybrid, the signal was mixed with 15.5 dBm local oscillator (LO) light from an external-cavity laser (ECL) with a linewidth of 100 kHz. The beating outputs were passed through four balanced photodetectors. A 4-channel real-time oscilloscope sampled the signal at a sampling rate of 80 GSa/s and digitized it with 8-bit resolution.

Fig. 2 shows the top-level block diagram of the receiver. The DSP code starts with optical front-end compensation, including the DC removal, IQ imbalance compensation and optical hybrid IQ orthogonalization using the Gram-Schmidt orthogonalization procedure [10]. Next, the signal was resampled to two samples per symbol and then passed through the overlap-and-save frequency domain CD compensation and laser frequency offset compensation based on the FFT of the signal at the fourth power. Matched filtering was performed in the frequency domain using the same pulse-shaping filter used at the transmitter. Sampling frequency-offset compensation and timing recovery were carried out using a non-data-aided feed-forward symbol-timing estimator [11]. Next, synchronization is performed in order to facilitate data

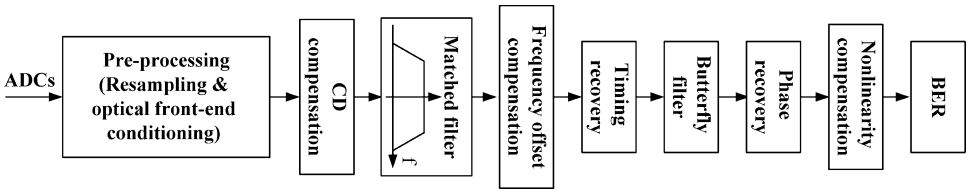

Fig. 2. Receiver DSP.

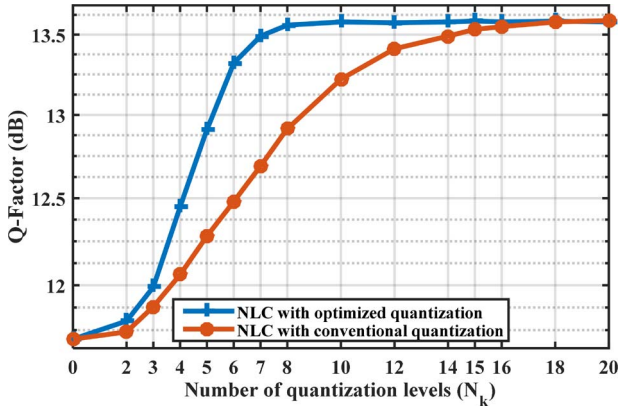

Fig. 3. Q-factor after nonlinearity compensation with optimized and linear quantization of perturbation coefficients.

aided modulation transparent equalization. A training-symbol-aided decision directed least radius distance [12] based fractionally spaced linear equalizer with 15 taps was used for fast convergence of the coefficients. The carrier phase was recovered using the superscalar parallelization based phase locked loop combined with a maximum likelihood phase estimation [13]. Next and for comparison purposes, the fiber nonlinearity is compensated using either our novel adaptive nonlinear equalizer or the linearly quantized perturbation based post nonlinearity compensation technique. Finally, the symbols were mapped to bits and the bit error rate (BER) was counted over 100,000 bits and a soft-decision forward error correction (20% overhead) BER threshold of 2×10^{-2} was considered.

5. Results

Fig. 3 shows the Q-factor after 2560 km SMF transmission for different numbers of quantization levels at the optimum nonlinear launch power, which is equal to 1 and 2 dBm for linear and optimized techniques, respectively (as shown in Fig. 4). For five quantization levels, our optimized quantization method outperforms conventional linear quantization by more than 0.5 dB in terms of Q-factor improvement. With only eight levels, the DD-LMS based quantization scheme reaches its maximum performance and the nonlinearity compensation (NLC) gain increases slightly with more quantization levels. On the other hand, the linear method requires 15 quantization levels for the same NLC gain, and the Q-factor shows a stronger dependence on the number of quantization levels.

Fig. 4 shows Q-factor versus different launch powers after 2560 km. Here the number of quantization levels equals 8 for both the optimized and the linear quantization methods, and the optimum lunch power increases by 2 dBm for both nonlinearity compensation methods. In addition, the Q-factor improved by 0.85 and 0.3 dB and the nonlinearity tolerance improved by 2.2 and 3.35 dBm in the case of linear and optimized quantization of perturbation coefficients, respectively.

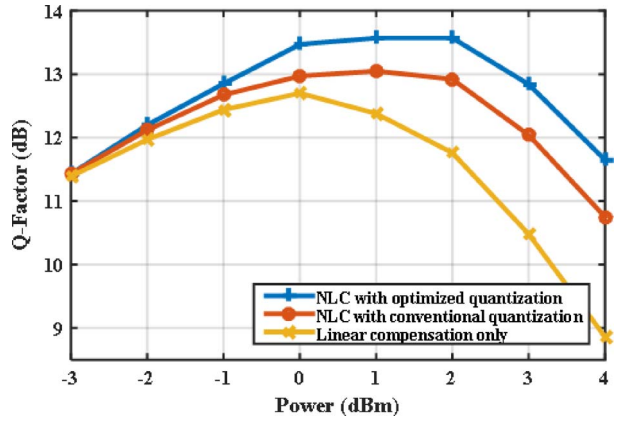

Fig. 4. Q-factor versus launch power for linear compensation and nonlinearity compensation with optimized and linear quantization of perturbation coefficients ($N_k = 8$).

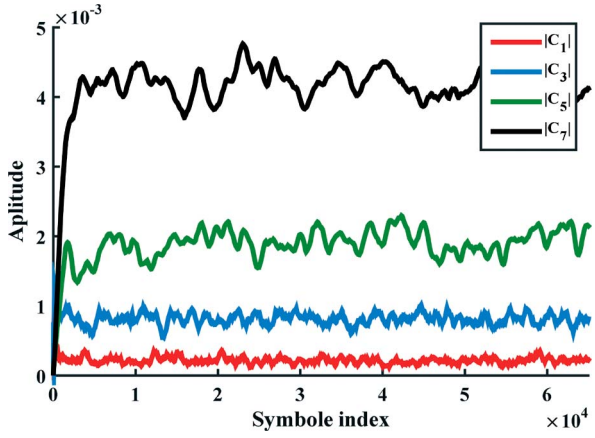

Fig. 5. Convergence of adaptive perturbation coefficients over time ($N_k = 8$).

Fig. 5 shows convergence of optimized quantized perturbation coefficients over time, when number of quantization levels equals 8. It can be seen that rapid convergence can be achieved even in the extreme case of initializing the DD-LMS algorithm with zeros. We point out that the nonlinear perturbation coefficients are not time varying, and therefore, adaptation of perturbation coefficients can be terminated after convergence is obtained. Subsequently, the average steady-state perturbation coefficient values can be used for nonlinear compensation, and these optimum coefficients can be stored in the memory for future use.

6. Conclusion

In order to further reduce the complexity and simplify implementation, we propose a decision directed least mean square (DD-LMS) algorithm for optimization of quantized perturbation coefficients for the fiber nonlinearity compensation. Our method shows robust tolerance to aggressive quantization. We have experimentally demonstrated that the number of quantization levels can be reduced from 15 to eight after 2560 km single mode fiber transmission when compared to the conventional linear quantization scheme.

Acknowledgment

The authors wish to thank Dr. I. Tselniker for his valuable suggestions.

References

[1] R. Dar, M. Shtaif, and M. Feder, "New bounds on the capacity of the nonlinear fiber-optic channel," *Opt. Lett.*, vol. 39, no. 2, pp. 398–401, Jan. 2014.

[2] D. Rafique, J. Zhao, and A. D. Ellis, "Digital back-propagation for spectrally efficient WDM 112 Gbit/s PM m-ary QAM transmission," *Opt. Exp.*, vol. 19, no. 6, pp. 5219–5224, Mar. 2011.

[3] Y. Gao, J. H. Ke, K. P. Zhong, J. C. Cartledge, and S. S.-H. Yam, "Assessment of intrachannel nonlinear compensation for 112 Gb/s dual-polarization 16QAM systems," *J. Lightw. Technol.*, vol. 30, no. 24, pp. 3902–3910, Dec. 2012.

[4] Z. Tao *et al.,* "Multiplier-free intrachannel nonlinearity compensating algorithm operating at symbol rate," *J. Lightw. Technol.*, vol. 29, no. 17, pp. 2570–2576, Sep. 2011.

[5] Z. Li, W.-R. Peng, F. Zhu, and Y. Bai, "MMSE-based optimization of perturbation coefficients quantization for fiber nonlinearity mitigation," *J. Lightw. Technol.*, vol. 33, no. 20, pp. 4311–4317, Oct. 2015.

[6] M. Malekiha, I. Tselniker, and D. V. Plant, "Efficient nonlinear equalizer for intra-channel nonlinearity compensation for next generation agile and dynamically reconfigurable optical networks," *Opt. Exp.*, vol. 24, no. 4, pp. 4097–4108, Feb. 2016.

[7] G. P. Agrawal, *Fiber-Optic Communication Systems*. New York, NY, USA: Wiley, 1997.

[8] F. P. Guiomar, J. D. Reis, A. L. Teixeira, and A. N. Pinto, "Mitigation of intra-channel nonlinearities using a frequency-domain Volterra series equalizer," *Opt. Exp.*, vol. 20, no. 2, pp. 1360–1369, Jan. 2012.

[9] Y. Gao, F. Zhang, L. Dou, Z. Chen, and A. Xu, "Intra-channel nonlinearities mitigation in pseudo-linear coherent QPSK transmission systems via nonlinear electrical equalizer," *Opt. Commun.*, vol. 282, no. 12, pp. 2421–2425, Jun. 2009.

[10] S. J. Savory, "Digital coherent optical receivers: Algorithms and subsystems," *IEEE J. Sel. Topics Quantum Electron.*, vol. 16, no. 5, pp. 1164–1179, Sep./Oct. 2010.

[11] S. J. Lee, "A new non-data-aided feedforward symbol timing estimator using two samples per symbol," *IEEE Commun. Lett.*, vol. 6, no. 5, pp. 205–207, May 2002.

[12] X. Xu, B. Châtelain, and D. V. Plant, "Decision directed least radius distance algorithm for blind equalization in a dual-polarization 16-QAM system," in *Proc. OFC*, 2012, pp. 1–3.

[13] Q. Zhuge *et al.,* "Pilot-aided carrier phase recovery for M-QAM using superscalar parallelization based PLL," *Opt. Exp.*, vol. 20, no. 17, pp. 19599–19609, Aug. 2012.